STEM CELLS TRANSLATIONAL MEDICINE®

TISSUE ENGINEERING AND REGENERATIVE MEDICINE

Chondroitin Sulfate Glycosaminoglycan Scaffolds for Cell and Recombinant Protein-Based Bone Regeneration

SETH ANDREWS [a,b,*] ALBERT CHENG,[c,d,*] HAZEL STEVENS,[c] MEGHAN T. LOGUN,[a,e] ROBIN WEBB,[a] ERIN JORDAN,[a] BOAO XIA,[c] LOHITASH KARUMBAIAH,[a,f] ROBERT E. GULDBERG,[c,d] STEVEN STICE[a,f]

[a]Regenerative Bioscience Center, University of Georgia, Athens, Georgia, USA; [b]College of Engineering, University of Georgia, Athens, Georgia, USA; [c]George W. Woodruff School of Mechanical Engineering, Georgia Institute of Technology, Atlanta, Georgia, USA; [d]Parker H. Petit Institute for Bioengineering & Bioscience, Georgia Institute of Technology, Atlanta, Georgia, USA; [e]Biomedical Health Sciences Institute, University of Georgia, Athens, Georgia, USA; [f]Department of ADS, College of Agriculture and Environmental Science, University of Georgia, Athens, Georgia, USA

[*]Contributed equally

Correspondence: Steven Stice, Ph.D., Regenerative Bioscience Center, University of Georgia, Athens 30602, Georgia, USA. Telephone: 706.583.0071; e-mail: sstice@uga.edu

Received June 29, 2018; accepted for publication December 6, 2018; first published January 21, 2019.

http://dx.doi.org/10.1002/sctm.18-0141

Key Words. Bone morphogenetic protein-2 • Osteogenesis • Mesenchymal stromal cells • Chondroitin sulfate glycosaminoglycan • Genetic therapy

ABSTRACT

Bone morphogenetic protein 2 (BMP-2)-loaded collagen sponges remain the clinical standard for treatment of large bone defects when there is insufficient autograft, despite associated complications. Recent efforts to negate comorbidities have included biomaterials and gene therapy approaches to extend the duration of BMP-2 release and activity. In this study, we compared the collagen sponge clinical standard to chondroitin sulfate glycosaminoglycan (CS-GAG) scaffolds as a delivery vehicle for recombinant human BMP-2 (rhBMP-2) and rhBMP-2 expression via human *BMP-2* gene inserted into mesenchymal stem cells (BMP-2 MSC). We demonstrated extended release of rhBMP-2 from CS-GAG scaffolds compared to their collagen sponge counterparts, and further extended release from CS-GAG gels seeded with BMP-2 MSC. When used to treat a challenging critically sized femoral defect model in rats, both rhBMP-2 and BMP-2 MSC in CS-GAG induced comparable bone formation to the rhBMP-2 in collagen sponge, as measured by bone volume, strength, and stiffness. We conclude that CS-GAG scaffolds are a promising delivery vehicle for controlling the release of rhBMP-2 and to mediate the repair of critically sized segmental bone defects. STEM CELLS TRANSLATIONAL MEDICINE *2019;8:575–585*

SIGNIFICANCE STATEMENT

To the authors' knowledge, this study describes, for the first time, the use of chondroitin sulfate glycosaminoglycan (CS-GAG) as a scaffold for genetically engineered stem cells to heal a large bone defect. The study compares how bone morphogenetic protein 2 (BMP-2) is released from CS-GAG containing genetically modified stem cells, unmodified stem cells, or the BMP-2 protein itself and collagen containing BMP-2. Additionally, these methods were applied to a rigorous bone defect model and found that engineered stem cells in CS-GAG perform comparably to the current gold standard and much better than unmodified cells in CS-GAG. Results provide a comparison of varying bone repair techniques not often directly compared and demonstrate the usefulness of CS-GAG in BMP-2 release and its suitability for bone repair.

INTRODUCTION

Bone tissue is well-known for its remarkable healing abilities, but there are instances in which these mechanisms are insufficient on their own. Large defects or gaps in the bone are unable to be bridged without intervention. Allografts and autografts are popular bone grafting methods, accounting for over 2 million procedures per year [1]. However, these procedures are not devoid of complications. Autografts, which are derived from the patient themselves, are the current gold standard but are the most difficult to obtain and have the risk of donor site morbidity [2, 3]. Allografts, from other individuals of the same species, are more likely to be rejected, require lifelong immunosuppression, and are potential sources of disease transmission [2, 4, 5]. Because of these issues, there have been numerous attempts to develop new synthetic bone graft substitutes to enhance bone healing.

Bone morphogenetic protein 2 (BMP-2) is an osteoinductive growth factor commonly used in bone substitute applications. It usually exists as a homodimer, binding to serine/threonine kinase receptors to initiate endocrine, paracrine, and autocrine effects [6, 7]. The recombinant human BMP-2 (rhBMP-2) is Food and Drug Administration (FDA) approved and used clinically in combination with a collagen sponge.

It has been shown to reduce the rate of secondary intervention and enhance fracture healing and has shown additional benefits for many orthopedic applications [8, 9]. Thus, any new modality for treating critically sized bone defects should undergo a rigorous investigation with comparison to current FDA-approved techniques, such as rhBMP-2 on collagen sponge.

Despite its well-documented ability to induce bone formation, rhBMP-2 has a very short half-life, leading to the use of supraphysiological doses by clinicians [10, 11]. Complications associated with delivery of rhBMP-2 clinically have been reported to include ectopic bone formation, inflammation, and increased cancer rates among patients [12, 13]. Additionally, the large amount of recombinant protein required for this approach leads to increased costs compared with alternative treatments [14]. In rats, clinically relevant doses of rhBMP-2 have been shown to induce the formation of structurally abnormal bone, as well as inflammation [15]. These drawbacks could be addressed by using a delivery method with sustained release of a lower dose of BMP-2. One such delivery system could involve use of constitutive BMP-2 expression via genetically engineered mesenchymal stem cells (MSCs) for BMP-2 delivery (BMP-2 MSC) [16–19].

MSCs are multipotent stromal cells commonly studied and used for their ability to differentiate into the bone, cartilage, and adipose tissue [20]. They are attractive as a delivery mechanism because of their ease of collection and expansion from the bone marrow and adipose and umbilical tissues, as well as their immune modulation capabilities and allogeneic tolerability. Osteogenic differentiation can be readily induced in MSCs, even in the absence of BMP-2 and transforming growth factor β1 (TGF-β1) signaling [21]. Our group has previously demonstrated success in creating ectopic bone and regenerating critically sized defects in rats using BMP-2-expressing MSCs encapsulated in poly(ethylene glycol) (PEG) microspheres [22, 23]. However, these studies noted a sharp decrease in encapsulated cell viability after 4 days [22]. PEG has been shown to be safe for implantation, but it is not inherently osteoconductive or biodegradable without further modifications [24, 25]. In addition, PEG cell encapsulation procedures can be labor intensive, variable, and inefficient [26].

Chondroitin sulfate glycosaminoglycans (CS-GAGs) are found attached to CS proteoglycans in the extracellular matrix of the cartilage, bone, and other tissues. They are O-linked glycans consisting of repeating glucuronic acid and *N*-acetylgalactosamine disaccharides. CS-GAGs are important for the bone development as they can support osteogenesis and suppress bone resorption [21, 27–30]. Additionally, they regulate both TGF-β1 and BMP signaling in bone and have been shown to retain TGF-β [21, 31]. In other studies, sulfated GAGs assisted in BMP-2's interaction with its receptor and oversulfated chondroitin sulfate-enhanced osteoblast mineralization in the presence of BMP-4 [32, 33]. These qualities lend themselves to the use of CS-GAGs as a scaffold for the slow release of BMP-2.

In this study, we describe an injectable biologic therapy for large bone defect healing. It consists of human MSCs genetically engineered to overexpress BMP-2, which are then seeded in a CS-GAG hydrogel. To increase retention of the therapeutic within the bone defect, we delivered the hydrogels in electrospun polycaprolactone nanofiber meshes, which have been previously demonstrated by members of our group to enhance hydrogel-mediated BMP-2 delivery [34]. We demonstrated high levels of BMP-2 expression in BMP-2 MSCs, maintained viability postseeding, and sustained in vitro BMP-2 release from this system compared to BMP-2 on collagen sponge. Additionally, we show the formation of comparable bone quantity and quality to the clinical standard in a rigorous rodent critically sized segmental defect model. These results indicate the potential of this system to be a valuable therapeutic option for healing large bone defects.

METHODS

Cell Culture and Transduction

Because of the differences in MSC behavior as a result of tissue source, both human umbilical (uMSC) and bone marrow MSCs (bmMSC; Lifeline Cell Technology, Frederick MD, Sciencell, Carlsbad, CA; one donor each) were used [35]. Both MSC types were plated at 5,000 cells per cm^2 on tissue culture flasks in complete medium, α-minimum essential medium (MEM-α), 10% defined fetal bovine serum (Hyclone, South Logan, UT), 2 mM L-glutamine, 50 U/ml penicillin, and 50 μg/ml streptomycin and allowed to grow to 80%–90% confluence (20,000–25,000 cells per cm^2). To transduce for BMP or Red Fluorescent Protein (RFP) expression, cells were harvested using 0.05% trypsin and plated at 26,000 cells per cm^2 in MEM-α, 10% defined fetal bovine serum, 5 μg/ml polybrene (Sigma-Aldrich, St. Louis, MO), and the appropriate multiplicity of infection (MOI) of *prEF1a-BMP-2* or *prEF1a-RFP* lentivirus (Cellecta, Mountain View, CA) on tissue culture flasks. The medium was changed back to complete medium 24 hours post-transduction. All cultures were maintained at 37°C and 5% CO_2. Cells that had undergone up to 20 passages were used in the generation of Figure 1's data, whereas all subsequent data were generated from cells that had undergone less than 10 passages. All materials were from Invitrogen (Carlsbad, CA) unless otherwise stated.

In Vitro RFP Expression

Following transduction of uMSCs and bmMSCs with the *prEF1a-RFP* vector in MOIs of 0, 1, 10, and 50 as described above, both phase contrast and fluorescent images were taken. Five images per well and three wells per condition were taken at 24, 48, and 72 hours post-transduction.

In Vitro BMP-2 Expression

Following transduction of bmMSCs or uMSCs with the *prEF1a-BMP-2* vector in MOIs of 10 and 50 as described above, 0.5 ml medium samples were collected in triplicate from different sets of wells at 48, 72, 96, and 120 hours post-transduction. BMP-2 concentrations were determined via BMP-2 enzyme-linked immunosorbent assay (ELISA; R&D Systems, Minneapolis, MN).

Hydrogel Preparation and Characterization

The CS-GAG hydrogels were created as previously described [36]. Briefly, hydrogel mixture was prepared by reconstituting 3% w/v of lyophilized methacrylated chondroitin sulfate and 0.01% 2-hydroxy-4′-(2-hydroxyethoxy)-2-methylpropiophenone (Irgacure-2959, Sigma-Aldrich, St. Louis, MO) in phosphate-buffered saline (PBS). These gels are polyanionic and have been shown to consist of 86% CS-A (4-sulfated), 6% CS-E (4,6-sulfated), 5% CS-C (6-sulfated), and unsulfated CS [36].

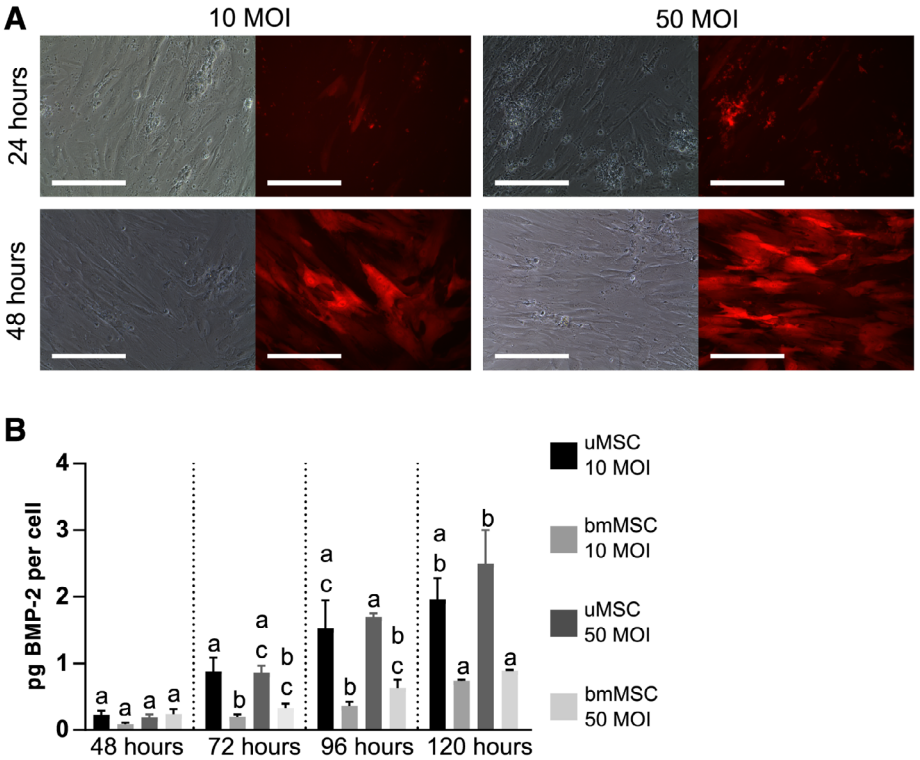

Figure 1. Efficient transduction of mesenchymal stem cells with a lentiviral vector at 10 MOI. **(A):** Images of uMSC over 72 hours after transducing with *prEF1α-RFP* at 10 and 50 MOI under phase contrast and RFP filter to evaluate transduction efficiency. Scale bars indicate 200 μm. $N = 15$. **(B):** Mean BMP-2 expression in uMSCs and bmMSCs at 48, 72, 96, and 120 hours after transducing with *prEF1α-BMP2* at 10 and 50 MOI, comparing expression over cell type and MOI within each time point. Transductions at 0 MOI did not result in BMP-2 expression detectable by BMP-2 enzyme-linked immunosorbent assay. Groups with differing letters are significantly different from each other within a time point at $p < .05$. Error bars indicate standard error. Two-way analysis of variance with Tukey's multiple comparison test ($n = 5–6$). Abbreviations: bmMSC, bone marrow mesenchymal stem cell; BMP-2, bone morphogenetic protein 2; MOI, moment of inertia; uMSC, umbilical mesenchymal stem cell.

Rheological testing of the hydrogel was performed as described previously [36]. Briefly, 500 μl of the hydrogel mixture was dispensed into a polydimethylsiloxane mold overlaid onto a glass slide and exposed to 365 nm long-wavelength UV light (160 W BlakRay, UVP, Upland, CA) for 3 minutes to yield hydrogel disks 1 inch in diameter and 6 mm thick. The hydrogels were then overlaid with 1 ml of PBS to swell overnight before rheological testing, which was performed on an ARES rheometer (TA Instruments, New Castle, DE), using a parallel plate geometry. Frequency sweep experiments from 0.1 to 100 Hz were performed at 5% strain at 25°C ($n = 5$) and storage modulus (Pa) versus angular frequency (rad/s) was plotted. Similarly, the dynamic viscosity and shear stress of the hydrogels were measured and viscosity (Pa s) and shear stress (Pa) versus shear rate (S^{-1}) were plotted.

Morphology of gold-coated lyophilized hydrogel samples was examined as described previously using a Zeiss 1450EP scanning electron microscope (SEM; Carl Zeiss, Oberkochen, Germany) [36]. Briefly, hydrogels were flash frozen in liquid nitrogen and lyophilized. We have not observed any discernible difference in structure and porosity of lyophilized snap frozen CS-GAG hydrogels reported in this study to hydrogels frozen overnight at −80°C as reported by us previously [36, 37]. They were then mounted on 10 mm SEM stubs and sputter coated (Structure Probe Inc., West Chester, PA) with gold for 30 seconds and imaged under an accelerated voltage of 5 kV. Images were acquired at ×165 and ×500 to observe the porosity and microstructure of the hydrogels.

Cell Seeding

Following casting as described above, 500 μl gels were frozen overnight at −80°C, after which they were lyophilized for 24 hours (Fig. 3A). To rehydrate them, the lyophilized hydrogels were overlaid with either a 6.66×10^6/mL cell suspension (GAG + MSC or GAG + BMP-2 MSC) or 33.3 μg/ml rhBMP-2 (GAG + rhBMP-2) of equal volume to the gel in MEM-α and allowed to incubate at 37°C and 5% CO_2 until all free liquid was absorbed into the gel. The hydrogel was then transferred to a sterile 1-ml syringe, pulse centrifuged to remove air pockets, and injected/ejected with a sterile 22G needle.

Viability and Distribution

Twenty-four hours after transduction with the prEF1a-RFP vector at MOI 10, uMSCs were seeded in CS-GAG hydrogels and overlaid with 2 μM calcein in PBS ($n = 5$). Nonfluorescent calcein AM was hydrolyzed to fluorescent calcein in live cells by the action of intracellular esterases. Cells were imaged using Fluorescein isothiocyanate (FITC) and Tetramethylrhodamine (TRITC) fluorescent filters 3 hours after seeding. Viability of transduced cells was determined by quantifying the degree of fluorescence overlap of RFP and calcein using the Mander's overlap coefficient

parameters in Volocity (PerkinElmer, Waltham, MA) as described previously [37].

Nanofiber Mesh Fabrication

Perforated nanofiber mesh tubes were fabricated as described previously [34]. A 12% (w/v) solution of poly(ε-caprolactone) (PCL) was made by dissolving PCL (Sigma-Aldrich, St. Louis, MO) in a 90:10 mixture of hexafluoro-2-propanol:dimethylformamide (Sigma-Aldrich, St. Louis, MO). The solution (∼4 ml) was electrospun onto a static collector plate to obtain PCL sheets. Rectangular sections (12 × 19 mm) containing twenty-three 1-mm-diameter circular holes were then cut using a VLS3.50 laser cutter (Universal Laser Systems, Scottsdale, AZ). Each rectangular piece was then rolled up into a cylindrical tube (5 mm diameter and 12 mm in length) and glued using medical grade UV-curable adhesive (Dymax, Torrington, CT). Meshes were sterilized by ethanol evaporation, washed and stored in PBS, and then transferred to MEM-α and stored at 4°C prior to use.

Preparation of GAG Treatment Groups

One day before surgery/experiment, uMSCs were either left nontransduced or transduced at 10 MOI and seeded in CS-GAG hydrogels 24 hours after transduction as described above. On the day of surgery/experiment, rhBMP-2 (R&D Systems, Minneapolis, MN) was reconstituted according to the manufacturer's instructions, diluted to 33.3 μg/ml in MEM-α, and used to rehydrate lyophilized CS-GAG hydrogel as described above. This rhBMP-2 dose, equating to 5 μg per gel, has previously been demonstrated to be the ideal minimum does for defect bridging in this defect model with low risk of complications [38].

Collagen Sponge Preparation

The day before each surgery/experiment, rhBMP-2 (Pfizer Inc., New York, NY) in 0.1% rat serum albumin (Sigma-Aldrich, St. Louis, MO) in 4 mM HCl solution was made up to a concentration of 33.3 μg/ml and then stored at 4°C overnight. Collagen sponge cylinders ∼5 mm in diameter and 10 mm in length were created by biopsy punching out from a sheet of bovine collagen sponge (Kensey Nash/DSM, Exton PA). All collagen sponge cylinders were sterilized by ethylene oxide. Before the start of the surgery/experiment, the collagen sponge cylinders were transferred to a 24-well plate, and then 150 μl of the rhBMP-2 solution was slowly loaded onto each cylinder. The sponges were left to sit for ∼10 minutes to soak up any residual rhBMP-2 solution in the well before being carefully transferred to another well plate for in vitro release characterization or press-fit into the bone defect for in vivo studies.

Hydrogel BMP-2 Release

Experimental groups were prepared as follows: CS-GAG hydrogels were rehydrated with 6.67×10^6 cells per ml nontransduced uMSCs (GAG + MSC), transduced uMSCs (GAG + BMP-2 MSC), or 33.3 μg/ml rhBMP-2 (GAG + rhBMP-2), and 150 μl of each rehydrated gel was injected into PCL nanofiber meshes and placed into individual wells of an ultra-low adhesion 24-well plate (Nunclon Sphera, ThermoFisher, Waltham, MA). For the collagen sponge group (Col + rhBMP-2), 150 μl of 3.33 μg/ml rhBMP-2 solution was loaded onto each sponge, and each sponge was then placed into an individual well of the 24-well plate (without any PCL mesh).

For the release experiment, 1 ml of MEM-α only was added to each well (n = 3–4). All scaffolds were then allowed to incubate at 37°C and 5% CO_2. At 3 hours, 12 hours, and 1, 2, 3, 5, 7, 9, 11, and 13 days, the overlaid media were collected and immediately stored at −80°C, and the extracted medium was replaced with 1 ml of fresh medium. On day 15, the medium was collected and then replaced with 1 ml of digest solution. The CS-GAG hydrogels were digested with 1 ml medium containing 20 mU of chondroitinase ABC (Sigma-Aldrich, St. Louis, MO), whereas the collagen sponges were digested with 1 mg/ml collagenase type I (Sigma-Aldrich, St. Louis, MO). Digestion occurred for 24 hours at 37°C before collection and storage at −80°C as before. BMP-2 ELISA was performed on the collected medium to determine the amount of BMP-2 released from the scaffolds at each time point.

Segmental Defect Surgery

All surgical procedures were approved by the Georgia Institute of Technology Institutional Animal Care and Use Committee, and NIH standards for animal care were followed. This surgical procedure has been described previously [39]. Before surgery, all animals were given a subcutaneous injection of slow-release buprenorphine (ZooPharm, Windsor, CO) for analgesia, and anesthesia was induced and maintained using isoflurane (Henry Schein Animal Health, Dublin, OH) inhalation. Briefly, an anterolateral skin incision was made in the leg, and then blunt dissection was performed to allow for placement of a polysulfone fixation plate. Critically sized 8 mm defects were created in the mid-diaphysis of the femur using an oscillating saw. The desired therapeutic was then delivered to the defect site, and finally, the muscle and skin were closed using 4–0 vicryl suture (Ethicon, Somerville, NJ) and wound clips, respectively. While the collagen sponge was pressed fit in the defect space, for the rest of the groups, the PCL scaffold was first fitted over the ends of the femur, followed by injection of the hydrogel. For all experiments, 14-week-old female RNU nude rats (Charles River Laboratories, Wilmington, MA) were used. A total of 15 rats were used, which allowed for 30 total bone defects (bilateral femurs). The sample sizes for each group were as follows: GAG + MSC (n = 7), GAG + BMP-2 MSC (n = 7), GAG + rhBMP-2 (n = 8), and Col + rhBMP-2 (n = 8).

Radiography and Microcomputed Tomography

To qualitatively assess longitudinal bone regeneration, two-dimensional (2D) in vivo radiographs were taken using the MX-20 digital machine (Faxitron X-ray Corp, Tucson, AZ) at 2, 4, 8, and 12 weeks postsurgery. Radiographs were acquired using an exposure time of 15 seconds and energy at 25 kV. Bridging scores were assigned to each radiograph by two blinded investigators, where bridging was defined as contiguous bone spanning the entire defect space (connecting at least one cortex from each bone end). In instances of disagreement, a third blinded investigator served as tiebreaker.

New bone formation was quantitatively evaluated using three-dimensional (3D) microcomputed tomography (μCT) at 12 weeks postsurgery. Scans were performed using the vivaCT40 (Scanco Medical, Brüttisellen, Switzerland). ex vivo scans were performed at a 21 μm voxel size, 55 kVp voltage, and a 145 μA current. The volume of interest consisted of the central 6.36 mm

(303 slices) of the defect. A threshold corresponding to 50% of native cortical bone density was applied to segment bone mineral [40].

Mechanical Testing

Torsional testing to failure was performed as previously described [39]. Animals were euthanized by CO_2 inhalation at 12 weeks postsurgery. Femurs were then excised, wrapped in PBS-soaked gauze, and stored at −20°C until testing could be performed. On the day of testing, samples were thawed in a beaker of tap water, the surrounding soft tissues were excised, and the fixation plate was removed so that the native bone ends could be potted in Wood's metal (Alfa Aesar, Haverhill, MA). Potted femurs were then rotated at a rate of 3° per second until failure using the EnduraTEC ELF3200 axial/torsion testing system (Bose, Framingham, MA). Failure strength was determined by locating the failure (peak) torque within the first 60° of rotation. Torsional stiffness was calculated by finding the slope of the linear region before failure in the torque-rotation plot.

Statistical Analysis

Unless otherwise noted, all data were analyzed via nonparametric Kruskal-Wallis test with multiple comparisons made by Dunn's post-tests as appropriate using GraphPad Prism software. Significance was determined as $p < .05$.

Results

MSC Transduction

Fluorescence microscopy of *pr-EF1α-RFP* lentivirus transduced uMSCs qualitatively showed transduction efficiency at 24, 48, and 72 hours post-transduction. Visual transduction efficiency approached 100% at 10 and 50 MOI (Fig. 1A). BMP-2 ELISA of media collected from *pr-EF1α-BMP2* lentivirus transduced MSCs at 48, 72, 96, and 120 hours post-transduction assessed rhBMP-2 production in both uMSCs and bmMSCs at 10 and 50 MOI (Fig. 1B). Nontransduced MSCs expressed BMP-2 below the detection threshold of the ELISA kit used and are not shown. All transductions resulted in greater amounts of rhBMP-2 released over time. By 96 and 120 hours post-transduction, significantly more BMP-2 per cell was produced at both 10 and 50 MOI in uMSC than bmMSC. However, there was no significant difference between 10 and 50 MOI for either cell type.

CS Hydrogel Characterization

The 3% CS hydrogels were transparent and porous (Fig. 2A), with pores ranging between 20 and 100 μm in diameter. The hydrogel storage modulus ranged between 350 and 450 Pa, increased at higher frequencies indicating strain hardening, and demonstrated nonlinear elasticity that is typical of biological materials (Fig. 2B) [6]. Measurement of dynamic viscosity indicated a decrease in viscosity with increasing shear rate, reflecting shear thinning and pseudoplastic material properties that are characteristic of shear-rate-dependent breakage of interchain linkages in hydrogels (Fig. 2C). The shear stress versus shear rate plot indicates a dependence of shear stress on shear rate, especially at higher shear rate values suggesting that the hydrogel exhibits partially viscoplastic properties (Fig. 2C).

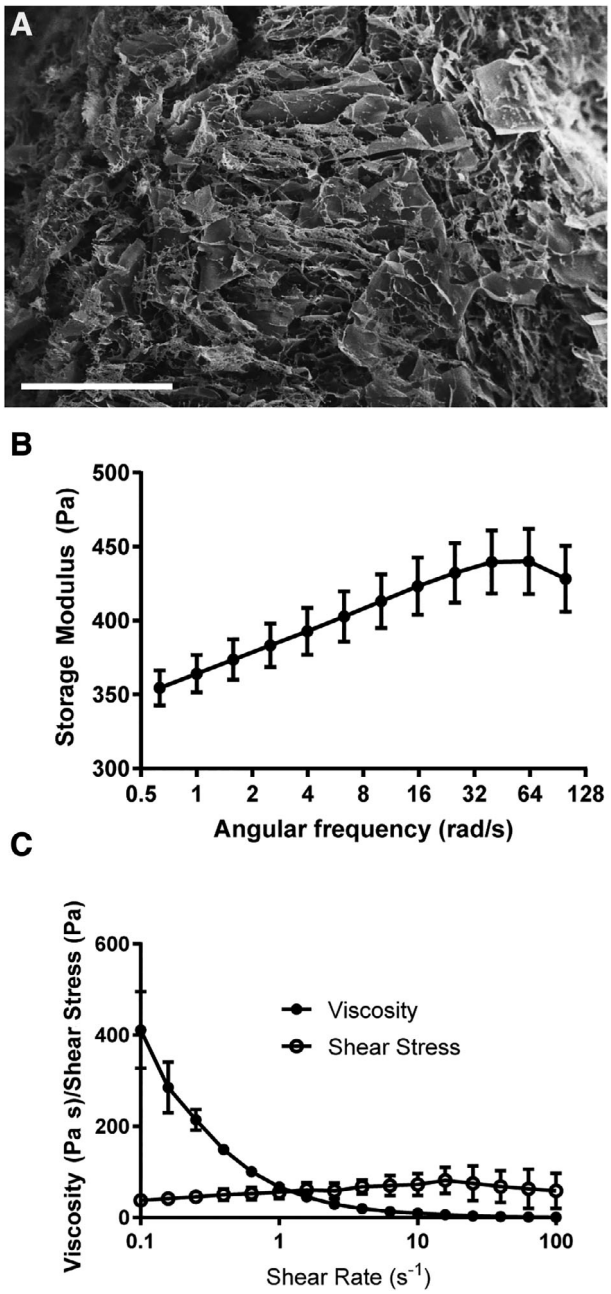

Figure 2. Chondroitin sulfate glycosaminoglycan (CS-GAG) hydrogel is porous with stable rheology. **(A):** Scanning electron microscopy of CS gel surface at ×165 magnification. Pore sizes are approximately 20–100 μm. Scale bar indicates 500 μm. **(B):** Rheology of CS-GAG gel. Data indicate stable rheological properties across a range of frequencies. **(C):** Dynamic viscosity decreases, and shear stress increases with an increase in shear rate. Error bars indicate standard error ($n = 5$).

Transduced MSC Viability and Distribution in CS Hydrogels

Viable transduced MSCs were identified via colocalization of RFP and calcein AM. Seeded MSCs were distributed homogeneously and showed colocalization of RFP and calcein in the cytoplasm. Ejection from the syringe had no effect on the viability of MSCs encapsulated within the gel (data not shown).

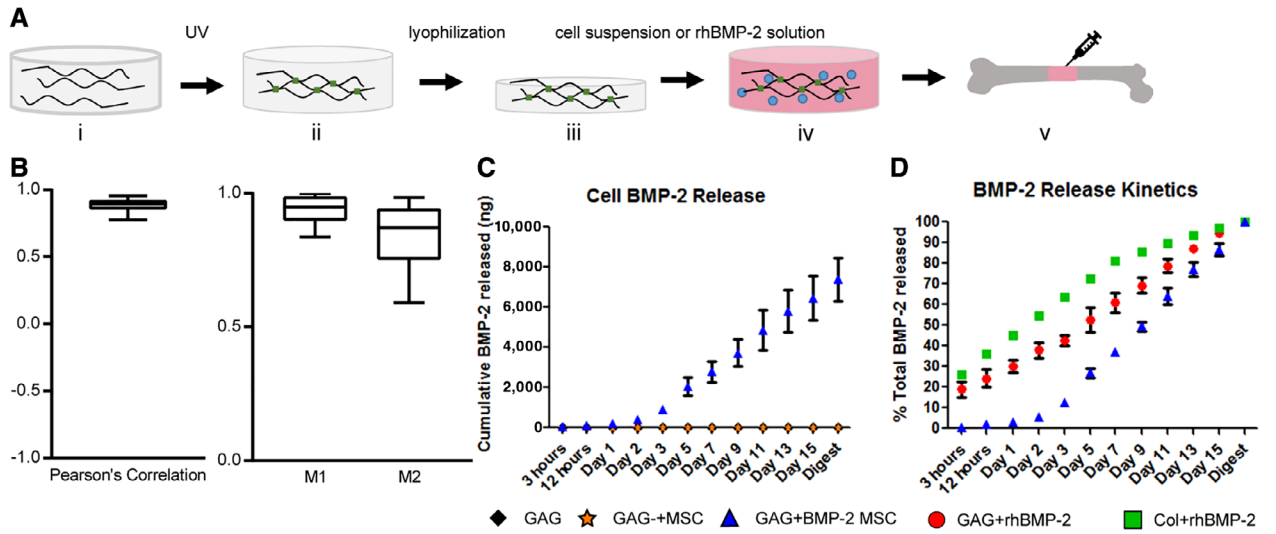

Figure 3. Preparation of chondroitin sulfate GAG hydrogel and interactions with transduced MSCs. **(A):** Casting of 3% GAG hydrogel (i) followed by photo crosslinking under UV light (ii). The hydrogel is lyophilized for 24 hours (iii) before it is rehydrated with a cell suspension in basal media (iv). **(B):** Measures of colocalization for calcein and RFP: Pearson's correlation, describing the extent of overlap between RFP and calcein images, and colocalization coefficients M1 and M2, describing the fraction of RFP colocalizing with calcein and the fraction of calcein localizing with RFP, respectively (n = 5). **(C):** Cumulative BMP-2 release over 15 days from empty GAG gels, GAG gels loaded with 1 million nontransduced MSCs, and GAG gels loaded with 1 million BMP-2 MSCs (n = 3–4). **(D):** BMP-2 release kinetics shown as percentage of the total amount released for GAG gels loaded with BMP-2 MSCs, as well as GAG gels and collagen sponges loaded with rhBMP-2 (n = 3–4). Abbreviations: BMP-2, bone morphogenetic protein 2; GAG, glycosaminoglycan; MSC, mesenchymal stem cell; rhBMP-2, recombinant human BMP-2.

Mean values and standard error of Pearson's correlation and colocalization coefficients M1 and M2 were 0.88 ± 0.01, 0.94 ± 0.01, and 0.85 ± 0.02, respectively, indicating approximately 85%–88% viability in seeded cells (Fig. 3B).

Quantification of BMP-2 Release

BMP-2 MSC in GAG hydrogel secreted over 7 μg of BMP-2 cumulatively over the course of 16 days in vitro, which was over ×1,000 higher than the release from nontransduced MSCs in GAG in the same time period (Fig. 3C). Furthermore, comparison of the release kinetics to exogenous delivery of rhBMP-2 revealed that Col + rhBMP-2 had the highest initial burst release of BMP-2, followed by GAG + rhBMP-2, and GAG + BMP-2 MSC having the slowest BMP-2 release profile (Fig. 3D). The time taken to release 50% of the total BMP-2 was approximately day 1.5, day 5, and day 9 for Col + rhBMP-2, GAG + rhBMP-2, and GAG + BMP-2 MSC, respectively.

Bone Defect Bridging

Radiographs qualitatively showed progressive mineralization from 4 to 12 weeks in the GAG + BMP-2 MSC, GAG + rhBMP-2, and Col + rhBMP-2 groups (Fig. 4B). Defect bridging was determined from the radiographs after 12 weeks, and the bridging scores for each group were 0/7 for GAG + MSC, 4/7 for GAG + BMP-2 MSC, 6/8 for GAG + rhBMP-2, and 7/8 for Col + rhBMP-2. These 2D assessments of defect bridging were verified using 3D μCT reconstructions as well (Fig. 4C).

Bone Formation Quantification

μCT analysis showed mean total bone volumes of 2.81, 42.91, 44.52, and 39.70 mm^3, respectively, in the GAG + MSC, GAG + BMP-2 MSC, GAG + rhBMP-2, and Col + rhBMP-2 groups at 12 weeks (Fig. 5A). Bone volumes in the GAG + MSC group were significantly lower than that of the other three groups. There were no significant differences in bone volume among GAG + BMP-2 MSC, GAG + rhBMP-2, and Col + rhBMP-2. Interestingly, when polar MOI (pMOI) was calculated to assess the spatial distribution of the newly formed bone (Fig. 5B), both GAG + BMP-2 MSC and GAG + rhBMP-2 groups had significantly higher average pMOI compared to GAG + MSC, whereas Col + rhBMP-2 did not.

Biomechanical Testing

The mean failure torques were 0.0066, 0.1250, 0.1465, and 0.1774 newton (N) m, respectively, in the GAG + MSC, GAG + BMP-2 MSC, GAG + rhBMP-2, and Col + rhBMP-2 groups at 12 weeks (Fig. 5C). The mean torsional stiffnesses were 0.00009, 0.0149, 0.0159, and 0.0197 N m/deg, respectively, in the GAG + MSC, GAG + -2 MSC, GAG + rhBMP-2, and Col + rhBMP-2 groups (Fig. 5D). For both parameters, only the GAG + rhBMP-2 and Col + rhBMP-2 groups had significantly higher values compared to GAG + MSC. However, there were no significant differences among GAG + BMP-2 MSC, GAG + rhBMP-2, and Col + rhBMP-2 groups.

Histology

H&E staining demonstrated clear morphological differences between the three BMP-2 groups and the GAG + MSC group (Fig. 6A). In the GAG + MSC samples, there was very little new bone formation and instead, the defect was filled with mostly soft, fibrous-like tissue with extensive cell infiltrate. In contrast, the GAG + BMP-2 MSC, GAG + rhBMP-2, and Col rhBMP-2 groups all showed distinct islands of new bone formation that were surrounded by marrow-like material. In the Col + rhBMP-2 group in particular, this marrow-like material appeared less dense and much more disperse. When viewed under polarized light

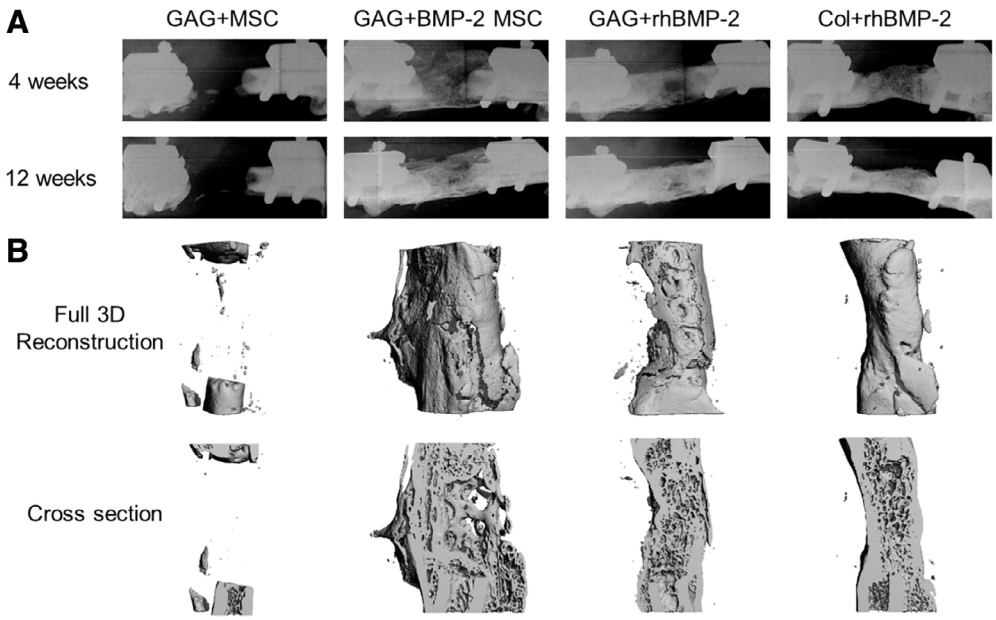

Figure 4. Defects bridge when treated with rhBMP-2 or BMP-2 MSCs. **(A):** Representative longitudinal radiographs at 4 and 12 weeks postsurgery. Defects were treated with 1 million nontransduced umbilical mesenchymal stem cells (uMSCs) in 150 μl chondroitin sulfate (CS)-GAG gel, 1 million BMP-2 uMSCs in 150 μl CS-GAG gel, 150 μl CS-GAG hydrogel loaded with 5 μg rhBMP-2, or 150 μL collagen sponge loaded with 5 μg rhBMP-2. **(B):** Twelve-week micro-computed tomography reconstructions of the same bone defects shown in the radiographs. Abbreviations: 3D, three dimension; BMP-2, bone morphogenetic protein 2; GAG, glycosaminoglycan; MSC, mesenchymal stem cell; rhBMP-2, recombinant human BMP-2.

(Fig. 6B), the collagen of the new bone in the Col + rhBMP-2 group appeared much more aligned (bright pink), indicative of lamellar structure, whereas the new bone in both GAG + BMP-2 MSC and GAG + rhBMP-2 groups had more disorganized collagen, suggestive of woven bone morphology.

Discussion

The complex milieu of cells, soluble factors and extracellular matrix at the bone defect site, is largely unexplored. However, treatment with substantial doses of rhBMP-2 at orthotopic sites can lead to robust bone healing. Given the complications that can arise from high-dose bolus rhBMP-2 treatment, alternative controlled delivery strategies have been sought, comprising cell and gene-based therapies within biomaterial carriers. Indeed rhBMP-2 genetically engineered MSCs have been shown to promote bone regeneration in a rat calvarial bone defect [41] and in mandible distraction surgery in dogs [42]. In previous studies, polymer scaffolds coated with adeno-associated viral vector encoding rhBMP-2 successfully bridged approximately 50% of rat femoral defects at 12 weeks without ectopic bone formation [43], and low-dose sustained rhBMP-2 expression was achieved by PEG-encapsulated rhBMP-2 expressing MSCs [23]. In the latter case, the use of a CS-GAG hydrogel could present additional advantages with sulfated CS-GAGs, promoting rhBMP-2 stabilization as demonstrated previously [32] and as discussed in our findings here.

In this study, we compared the collagen sponge clinical standard to CS-GAG as a delivery vehicle for rhBMP-2 and rhBMP-2 expression via rhBMP-2 gene inserted into MSCs (BMP-2 MSC). As the lentiviral system is able to integrate into the host cell genome, MSCs were transduced with a lentiviral vector to express high levels of rhBMP-2, with MSCs sourced from umbilical tissue expressing at a higher level than those from bone marrow. The uMSCs were therefore used in the subsequent experiments. Most previous studies have used bmMSCs, but Mizrahi et al. showed similar efficiency of BMP overexpression between bone and adipose-derived MSCs [18, 44–46]. However, given that this study only used one donor from each cell type, any differences seen here should be attributed to differences between cell lines, rather than tissue sources. Alternatively, uMSCs have a higher proliferative potential than bmMSCs, together with differences in gene expression and secretome and a more optimal tissue source for BMP-2 overexpression [47]. Compared to previous studies using adenovirus or nucleofection, lentiviral transduction induced a higher expression of BMP and greater bone formation in vivo [23, 33, 48]. Our comparisons between adenoviral and lentiviral transduction within the same MSC population (not shown) corroborate these findings, prompting us to implant far fewer cells (only 1 million BMP-2 MSCs per defect) than similar studies.

The characterization of the in vitro rhBMP-2 release profiles permitted greater insights into the potential differences in bone regeneration in vivo. Of the three rhBMP-2 treatment groups tested (GAG + BMP-2 MSC, GAG + rhBMP-2, and Col + rhBMP-2), Col + rhBMP-2 demonstrated the fastest initial burst release, whereas GAG + BMP-2 MSC exhibited the slowest, most sustained release. We expect the CS-GAG to be degraded over the course of 2 weeks, while the collagen sponge will persist for longer [36]. However, given the very short half-life of BMP-2 in vivo, we expect that this shorter degradation time for CS-GAG will not have much bearing on the release of active BMP-2 [49]. These in vitro observations were partially reflected in the spatial distribution of newly formed bone in vivo, as the GAG + BMP-2 MSC group had the

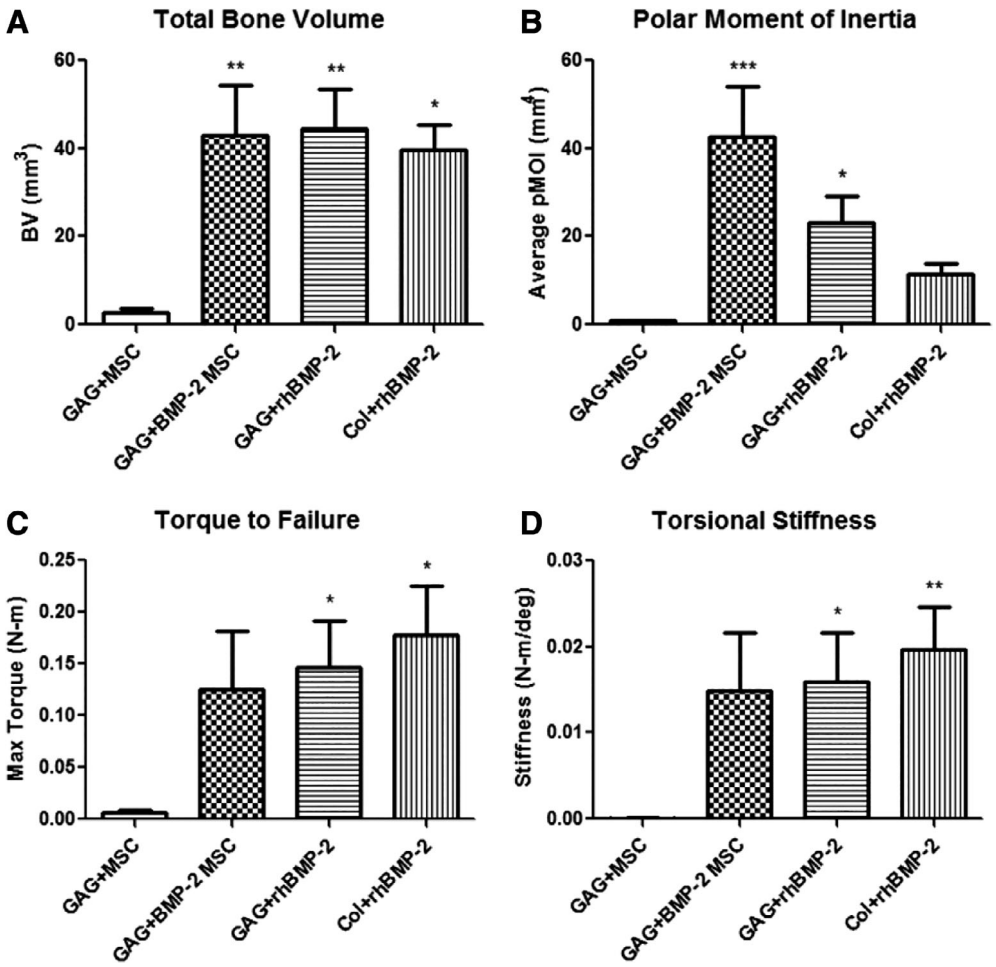

Figure 5. Newly formed bone similar between rhBMP-2 and BMP-2 MSC groups. Micro-computed tomography characterization and mechanical testing of regenerated femurs at 12 weeks. **(A):** Quantification of new bone revealed GAG + BMP-2 MSC, GAG + rhBMP-2, and Col + rhBMP-2 all demonstrated greater total BVs than GAG+MSC. **(B):** Calculated average pMOI showed that both GAG + BMP-2 MSC and GAG + rhBMP-2 groups had significantly higher pMOI compared to GAG + MSC. **(C):** Torque to failure. **(D):** Torsional stiffness measured from testing regenerated femurs to failure at 12 weeks. Both GAG + rhBMP-2 and Col + rhBMP-2 groups had significantly higher torque to failure and torsional stiffness compared to GAG + MSC. There were no significant differences among GAG + BMP-2 MSC, GAG + rhBMP-2, and Col + rhBMP-2 for any of these metrics. Error bars indicate standard error (n = 7–8 per group). Nonparametric Kruskal-Wallis test with multiple comparisons made by Dunn's post-tests. Abbreviations: BV, bone volume; BMP-2, bone morphogenetic protein 2; Col, collagen; GAG, glycosaminoglycan; MSC, mesenchymal stem cell; pMOI, polar moment of inertia; rhBMP-2, recombinant human BMP-2.

highest average pMOI, indicative of bone formation that is more disperse and peripheral. These results are in-line with findings from other groups, which have shown that the timing of rhBMP-2 expression/release greatly influences the distribution and quality of new bone formation. In particular, Koh et al. demonstrated that using a rapamycin-inducible system to generate more sustained rhBMP-2 release from delivered fibroblasts results in better mineralization compared to uncontrolled constitutive expression of rhBMP-2 [50]. Furthermore, histological characterization in our study revealed that the new bone formed in the Col + rhBMP-2 group had a lamellar-like structure, indicative of mature bone. This may suggest that the bone observed in the histological sections from the other two rhBMP-2 groups (GAG + BMP-2 MSC and GAG + rhBMP-2) had been deposited more recently and was possibly still actively (re)modeling at the 12-week time point. Interestingly, these observed differences in bone maturity and spatial distribution did not translate into functional differences between the three groups, in terms of the mechanical strength and stiffness of the regenerated femurs. A longer term study may enable newly formed bone in all groups to progress to a similar stage of maturation and consequently result in quantifiable mechanical differences. Overall, these results suggest that GAG + BMP-2 MSC delivery remains a viable treatment strategy which is comparable to delivery of rhBMP-2 in collagen sponge in this pre-clinical model.

Although GAG + BMP-2 MSC did not perform significantly better than Col + rhBMP-2 in this study, it is still remarkable that sufficient rhBMP-2 was released to induce healing that was comparable to the 5 μg rhBMP-2 delivered on collagen sponge. The 5 μg dose was chosen because previous work from our group has demonstrated this to be the optimal healing dose in this rat segmental defect model [51]. However, we should acknowledge that this level of dosing is not reflective of clinical doses, which is often orders of magnitude higher (even after accounting for dose per weight) [52]. The cell suspension

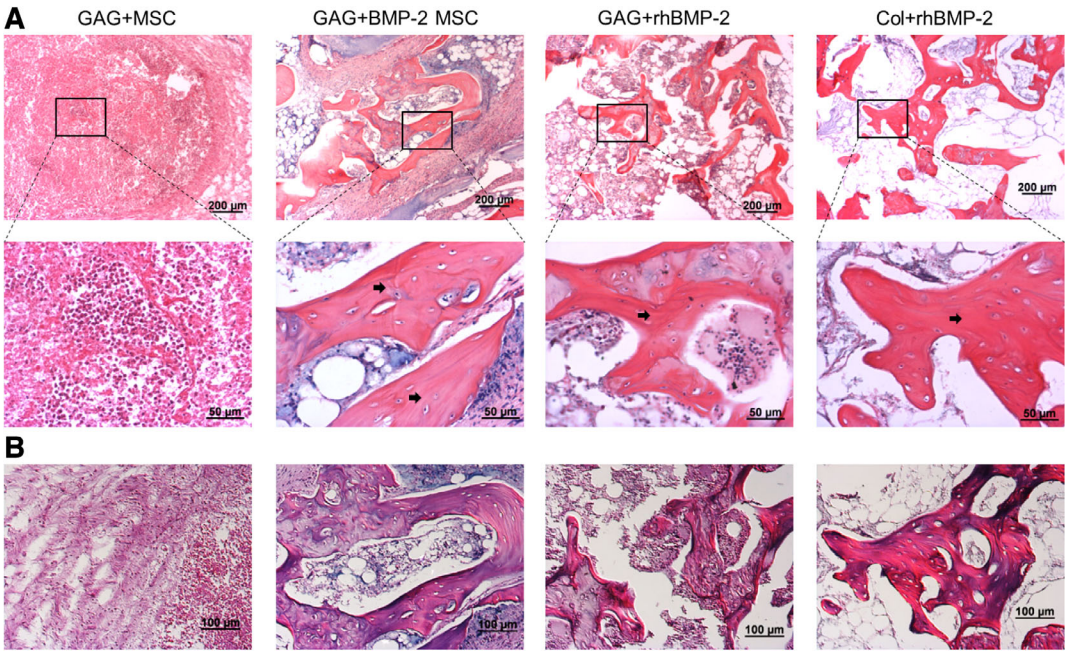

Figure 6. Histology reveals qualitative differences in bone maturity. Representative H&E images of defect tissue at 12 weeks postsurgery. **(A):** All BMP-2 groups exhibited islands of new bone formation while GAG + MSC did not. New bone is denoted by the black arrows in the higher magnification inset. **(B):** Furthermore, upon inspection under polarized light to assess collagen alignment, the bone in the Col + rhBMP-2 group appeared to be predominantly lamellar in structure, whereas both GAG + BMP-2 MSC and GAG + rhBMP-2 had material resembling woven bone. All images were taken in the middle of the bone defect. Abbreviations: BMP-2, bone morphogenetic protein 2; Col, collagen; GAG, glycosaminoglycan; MSC, mesenchymal stem cell; rhBMP-2, recombinant human BMP-2.

is capable of producing up to 7 μg BMP-2 over 16 days in culture (Fig. 3C) but this is assuming that all cells survive implantation. In vivo release of BMP-2 by these cells is unknown. Recent work has shown that using higher doses of rhBMP-2 on collagen sponge in this model results in substantial ectopic bone formation [53], recapitulating one of the main adverse events associated with high-dose rhBMP-2 use clinically. It remains to be seen whether this GAG gel system, which we demonstrated here to exhibit more sustained release compared to collagen sponge, would perform better at higher, more clinically relevant doses of rhBMP-2.

These results add to a growing body of evidence concerning the importance of CS-GAG to bone formation and BMP-2 signaling. Although there has been some disagreement on the role of GAGs in BMP-2 release, the sustained BMP-2 release profile from CS-GAG as compared to collagen may be explained by CS-GAG sulfation [54, 55]. Wang et al. found that CS-modified collagen scaffolds were more hydrophilic and had greater surface energy than their unmodified counterparts, which they postulated contributed to higher initial release of rhBMP-2 in the first 8 hours [56]. This contrasts somewhat with the in vitro release we observed but may indicate that sulfated GAGs play a role in rhBMP-2 stabilization. The importance of GAG sulfation is further reinforced by Hintze et al., who showed that CS with a higher degree of sulfation interacted with rhBMP-2 more strongly than their less sulfated counterparts for the same concentration [32], indicating that GAGs contributed to conformational and thermodynamic stabilization of rhBMP-2 and as a result, enhanced rhBMP-2 signaling. This enhanced rhBMP-2 stabilization and signaling could help explain the presence of woven bone in defects treated with either CS-GAG group in our study.

Conclusion

To our knowledge, this is the first study to investigate the suitability of CS-GAG hydrogels for rhBMP-2 delivery and to mediate the regeneration of a critically sized bone defect. Beyond the collagen scaffolds used clinically, there are a host of scaffold materials under development for BMP delivery [57]. Members of our group have previously demonstrated similar success in this same model with an alginate hydrogel [58]. In a study comparing rhBMP-2 delivery by chitosan and hyaluronic acid hydrogels, Luca et al. showed greater bone formation by volume using hyaluronic acid, whereas the chitosan scaffold led to more mature bone [59]. Although both materials are polysaccharides, chitosan is positively charged and hyaluronic acid is negatively charged—likely influencing their interactions with the positively charged rhBMP-2. Of these materials, hyaluronic acid is the most chemically similar component to CS-GAG, with one of its key differences being a lack of sulfation. In a study examining rhBMP-2 release kinetics from hyaluronic acid, 100% of the protein was eluted within 1 week from a relatively slowly degrading gel [60], which reinforces CS-GAG's advantages as scaffold for slow release of rhBMP-2.

Our in vitro results demonstrated that the GAG + BMP-2 MSC system resulted in slower release compared to Col + rhBMP-2. Future studies could assess cumulative release at higher rhBMP-2 doses and more importantly, whether sustained

release at higher doses is actually beneficial. In addition, one of the main concerns associated with rhBMP-2 use clinically is a heightened and uncontrolled inflammatory response [12, 61]. Although this was not directly investigated in this study, MSC delivery may mitigate these risks, given MSCs have extensive immunomodulatory capabilities and can influence multiple immune cell types [62–65]. Future work exploring how MSC therapy may improve rhBMP-2-mediated bone healing by limiting adverse effects could be impactful for clinicians.

Finally, this GAG + BMP-2 MSC system could potentially be enhanced further through incorporation of cell-adhesive ligands. In the context of bone repair, the fibronectin motif Arginylglycylaspartic acid (RGD) [34] and the collagen-mimetic peptide GFOGER [66] have been shown to be effective in promoting new bone formation. These studies have demonstrated that including cell adhesion ligands in the biomaterial scaffold can improve healing for both rhBMP-2 delivery as well as cell delivery approaches. Shekaran et al. showed that GFOGER delivered with a low dose of rhBMP-2 actually increased recruitment of CD45−/CD90+ osteoprogenitor cells to a radial defect compared to collagen sponge with rhBMP-2 [67]. In addition, Moshaverinia et al. demonstrated that osteogenic differentiation of multiple types of MSCs was enhanced when the cells were encapsulated in RGD alginate microspheres compared to nonfunctionalized alginate [68]. For our study, we tested both rhBMP-2 and MSC delivery approaches with a nonfunctionalized GAG gel and observed comparable healing to collagen sponge with rhBMP-2. Based on these findings from other labs, it seems plausible that functionalizing our GAG gel with RGD or GFOGER in the future could potentially result in even better outcomes.

Acknowledgment

This work was supported by DARPA Grant W911NF-09-1-0040.

Author Contributions

S.A., A.C.: collection and/or assembly of data, data analysis and interpretation, manuscript writing, final approval of manuscript; H.S.: collection and/or assembly of data, data analysis and interpretation, final approval of manuscript; M.T.L., B.X.: collection and/or assembly of data; R.W.: collection and/or assembly of data, data analysis and interpretation; E.J.: collection and/or assembly of data, data analysis and interpretation, final approval of manuscript; L.K.: conception/design, provision of study material or patients, collection and/or assembly of data, data analysis and interpretation, final approval of manuscript; R.E.G.: conception/design, financial support, provision of study material or patients, collection and/or assembly of data, data analysis and interpretation, final approval of manuscript; S.S.: conception/design, financial support, provision of study material or patients, data analysis and interpretation, final approval of manuscript.

Disclosure of Potential Conflicts of Interest

The authors indicated no potential conflicts of interest.

References

1 Greenwald AS, Boden SD, Goldberg VM et al. Bone-graft substitutes: Facts, fictions, and applications. J Bone Joint Surg Am 2001, 83-A(suppl 2; Pt 2):98–103.

2 Toolan BC. Current concepts review: Orthobiologics. Foot Ankle Int. 2006;27(7): 561–566.

3 De Long WG, Einhorn TA, Koval K et al. Bone grafts and bone graft substitutes in orthopaedic trauma surgery: A critical analysis. J Bone Joint Surg Am 2007;89:649–658.

4 Laurencin C, Khan Y, El-Amin SF. Bone graft substitutes. Expert Rev Med Devices 2006;3:49–57.

5 Desai BM. Osteobiologics. Am J Orthop (Belle Mead NJ) 2007;36(suppl 4):8–11.

6 Rahman MS, Akhtar N, Jamil HM et al. TGF-beta/BMP signaling and other molecular events: Regulation of osteoblastogenesis and bone formation. Bone Res 2015;3:15005.

7 Balboni AL, Hutchinson JA, DeCastro AJ et al. ΔNp63α-mediated activation of bone morphogenetic protein signaling governs stem cell activity and plasticity in normal and malignant mammary epithelial cells. Cancer Res 2013;73:1020–1030.

8 Govender S, Csimma C, Genant HK et al. Recombinant human bone morphogenetic protein-2 for treatment of open tibial fractures: A prospective, controlled, randomized study of four hundred and fifty patients. J Bone Joint Surg Am 2002;84:2123–2134.

9 Gothard D, Smith EL, Kanczler JM et al. Tissue engineered bone using select growth factors: A comprehensive review of animal studies and clinical translation studies in man. Eur Cells Mater 2014;28:166–208.

10 Jones ALBR, Bosse MJ, Mirza SK et al. Recombinant human BMP-2 and allograft compared with autogenous bone graft for reconstruction of diaphyseal tibial fractures with cortical defects. J Bone Joint Surg Am 2006;88: 1431–1441.

11 Zhao BKT, Toyoda H, Takada T et al. Heparin potentiates the in vivo ectopic bone formation induced by bone morphogenetic protein-2. J Biol Chem 2006;281:23246–23253.

12 Tannoury CA, An HS. Complications with the use of bone morphogenetic protein 2 (BMP-2) in spine surgery. Spine J 2014;14:552–559.

13 Valdes MA, Thakur NA, Namdari S et al. Recombinant bone morphogenic protein-2 in orthopaedic surgery: A review. Arch Orthop Trauma Surg 2009;129:1651–1657.

14 Daniel S, Mulconrey M, Keith H et al. Bone morphogenetic protein (RhBMP-2) as a substitute for Iliac crest bone graft in multilevel adult spinal deformity surgery. Spine J 2008;33:2153–2159.

15 Zara JN, Siu RK, Zhang X et al. High doses of bone morphogenetic protein 2 induce structurally abnormal bone and inflammation in vivo. Tissue Eng Part A 2011;17:1389–1399.

16 Riew KD, Wright NM, Cheng S-L et al. Induction of bone formation using a recombinant adenoviral vector carrying the human BMP-2 gene in a rabbit spinal fusion model. Calcif Tissue Int 1998;63:357–360.

17 Jay Lieberman AD, Stevenson S, Wu L et al. The effect of regional gene therapy with bone morphogenetic protein-2-producing bone-marrow cells on the repair of segmental femoral defects in rats. J Bone Joint Surg 1999;81-A (7):905–917.

18 S-L Cheng JL, Wright NM, Lai C-F et al. In vitro and in vivo induction of bone formation using a recombinant adenoviral vector carrying the human BMP-2 gene. Calcified Tissue Int 2001;68:87–94.

19 Hiroyuki Tsuchida JH, Crawford E, Manske P et al. Engineered allogeneic mesenchymal stem cells repair femoral segmental defect in rats. J Orthop Res 2003;21:44–53.

20 Campana V, Milano G, Pagano E et al. Bone substitutes in orthopaedic surgery: From basic science to clinical practice. J Mater Sci Mater Med 2014;25:2445–2461.

21 Buttner M, Moller S, Keller M et al. Over-sulfated chondroitin sulfate derivatives induce osteogenic differentiation of hMSC independent of BMP-2 and TGF-beta1 signalling. J Cell Physiol 2013;228:330–340.

22 Mumaw J, Jordan ET, Sonnet C et al. Rapid heterotrophic ossification with cryopreserved poly(ethylene glycol-) microencapsulated BMP2-expressing MSCs. Int J Biomater 2012;2012:861794.

23 Sonnet C, Simpson CL, Olabisi RM et al. Rapid healing of femoral defects in rats with low dose sustained BMP2 expression from

PEGDA hydrogel microspheres. J Orthop Res 2013;31:1597–1604.

24 Nuttelman CR, Tripodi MC, Anseth KS. Synthetic hydrogel niches that promote hMSC viability. Matrix Biol 2005;24:208–218.

25 Lutolf MP, Lauer-Fields JL, Schmoekel HG et al. Synthetic matrix metalloproteinase-sensitive hydrogels for the conduction of tissue regeneration: Engineering cell-invasion characteristics. Proc Natl Acad Sci USA 2003;100:5413–5418.

26 Olabisi RM. Cell microencapsulation with synthetic polymers. J Biomed Mater Res A 2015;103:846–859.

27 Salbach-Hirsch J, Ziegler N, Thiele S et al. Sulfated glycosaminoglycans support osteoblast functions and concurrently suppress osteoclasts. J Cell Biochem 2014;115:1101–1111.

28 Koike T, Izumikawa T, Tamura J et al. Chondroitin sulfate-E fine-tunes osteoblast differentiation via ERK1/2, Smad3 and Smad1/5/8 signaling by binding to N-cadherin and cadherin-11. Biochem Biophys Res Commun 2012; 420:523–529.

29 Gualeni B, de Vernejoul MC, Marty-Morieux C et al. Alteration of proteoglycan sulfation affects bone growth and remodeling. Bone 2013;54:83–91.

30 Cortes M, Baria AT, Schwartz NB. Sulfation of chondroitin sulfate proteoglycans is necessary for proper Indian hedgehog signaling in the developing growth plate. Development 2009;136:1697–1706.

31 Lim JJ, Temenoff JS. The effect of desulfation of chondroitin sulfate on interactions with positively charged growth factors and upregulation of cartilaginous markers in encapsulated MSCs. Biomaterials 2013;34:5007–5018.

32 Hintze V, Samsonov SA, Anselmi M et al. Sulfated glycosaminoglycans exploit the conformational plasticity of bone morphogenetic protein-2 (BMP-2) and alter the interaction profile with its receptor. Biomacromolecules 2014;15:3083–3092.

33 Miyazaki T, Miyauchi S, Tawada A et al. Oversulfated chondroitin sulfate-E binds to BMP-4 and enhances osteoblast differentiation. J Cell Physiol 2008;217:769–777.

34 Kolambkar YM, Dupont KM, Boerckel JD et al. An alginate-based hybrid system for growth factor delivery in the functional repair of large bone defects. Biomaterials 2011;32:65–74.

35 Hass R, Kasper C, Böhm S et al. Different populations and sources of human mesenchymal stem cells (MSC): A comparison of adult and neonatal tissue-derived MSC. Cell Commun Signal 2011;9:12–12.

36 Karumbaiah L, Enam SF, Brown AC et al. Chondroitin sulfate glycosaminoglycan hydrogels create endogenous niches for neural stem cells. Bioconjug Chem 2015;26:2336–2349.

37 Logun MT, Bisel NS, Tanasse EA et al. Glioma cell invasion is significantly enhanced in composite hydrogel matrices composed of chondroitin 4- and 4,6-sulfated glycosaminoglycans. J Mater Chem B 2016;4:6052–6064.

38 Boerckel JD, Kolambkar YM, Dupont KM et al. Effects of protein dose and delivery system on BMP-mediated bone regeneration. Biomaterials 2011;32:5241–5251.

39 Oest ME, Dupont KM, Kong HJ et al. Quantitative assessment of scaffold and growth factor-mediated repair of critically sized bone defects. J Orthop Res 2007;25:941–950.

40 Duvall CL, Taylor WR, Weiss D et al. Impaired angiogenesis, early callus formation, and late stage remodeling in fracture healing of osteopontin-deficient mice. J Bone Miner Res 2007;22:286–297.

41 He X, Dziak R, Yuan X et al. BMP2 genetically engineered MSCs and EPCs promote vascularized bone regeneration in rat critical-sized calvarial bone defects. PLoS One 2013;8:e60473.

42 Castro-Govea Y, Cervantes-Kardasch VH, Borrego-Soto G et al. Human bone morphogenetic protein 2-transduced mesenchymal stem cells improve bone regeneration in a model of mandible distraction surgery. J Craniofac Surg 2012;23:392–396.

43 Dupont KM, Boerckel JD, Stevens HY et al. Synthetic scaffold coating with adeno-associated virus encoding BMP2 to promote endogenous bone repair. Cell Tissue Res 2012; 347:575–588.

44 Mizrahi O, Sheyn D, Tawackoli W et al. BMP-6 is more efficient in bone formation than BMP-2 when overexpressed in mesenchymal stem cells. Gene Ther 2013;20:370–377.

45 DA Lieberman JR, Stevenson S, Wu L et al. The effect of regional gene therapy with bone morphogenetic protein-2-producing bone-marrow cells on the repair of segmental femoral defects in rats. J Bone Joint Surg 1999;81:905–917.

46 Chang SC, Chung HY, Tai CL et al. Repair of large cranial defects by hBMP-2 expressing bone marrow stromal cells: Comparison between alginate and collagen type I systems. J Biomed Mater Res A 2010;94: 433–441.

47 Arutyunyan I, Elchaninov A, Makarov A et al. Umbilical cord as prospective source for mesenchymal stem cell-based therapy. Stem Cells Int 2016;2016:6901286.

48 Pelled G, Sheyn D, Tawackoli W et al. BMP6-engineered MSCs induce vertebral bone repair in a pig model: A pilot study. Stem Cells Int 2016;2016:6530624.

49 Zhao B, Katagiri T Fau-Toyoda H, Toyoda H Fau-Takada T et al. Heparin potentiates the in vivo ectopic bone formation induced by bone morphogenetic protein-2. 2006.

50 Koh JT, Ge C, Zhao M et al. Use of a stringent dimerizer-regulated gene expression system for controlled BMP2 delivery. Mol Ther 2006;14:684–691.

51 Kolambkar YM, Boerckel JD, Dupont KM et al. Spatiotemporal delivery of bone morphogenetic protein enhances functional repair of segmental bone defects. Bone 2011; 49:485–492.

52 Fu R, Selph S, McDonagh M et al. Effectiveness and harms of recombinant human bone morphogenetic protein-2 in spine fusion: A systematic review and meta-analysis. Ann Intern Med 2013;158:890–902.

53 Krishnan L, Priddy LB, Esancy C et al. Delivery vehicle effects on bone regeneration and heterotopic ossification induced by high dose BMP-2. Acta Biomater 2017;49:101–112.

54 Jiao X, Billings PC, O'Connell MP et al. Heparan sulfate proteoglycans (HSPGs) modulate BMP2 osteogenic bioactivity in C2C12 cells. J Biol Chem 2007;282:1080–1086.

55 Takada T, Katagiri T, Ifuku M et al. Sulfated polysaccharides enhance the biological activities of bone morphogenetic proteins. J Biol Chem 2003;278(44):43229–43235.

56 Wang Y, Zhang L, Hu M et al. Effect of chondroitin sulfate modification on rhBMP-2 release kinetics from collagen delivery system. J Biomed Mater Res A 2010;92:693–701.

57 Blackwood KA, Bock N, Dargaville TR et al. Scaffolds for growth factor delivery as applied to bone tissue engineering. Int J Polym Sci 2012;2012:1–25.

58 Krishnan L, Priddy LB, Esancy C et al. Hydrogel-based delivery of rhBMP-2 improves healing of large bone defects compared with autograft. Clin Orthop Relat Res 2015;473: 2885–2897.

59 Luca L, Rougemont AL, Walpoth BH et al. The effects of carrier nature and pH on rhBMP-2-induced ectopic bone formation. J Control Release 2010;147:38–44.

60 Patterson J, Siew R, Herring SW et al. Hyaluronic acid hydrogels with controlled degradation properties for oriented bone regeneration. Biomaterials 2010;31:6772–6781.

61 Ritting AW, Weber EW, Lee MC. Exaggerated inflammatory response and bony resorption from BMP-2 use in a pediatric forearm nonunion. J Hand Surg Am 2012;37:316–321.

62 Chiesa S, Morbelli S, Morando S et al. Mesenchymal stem cells impair in vivo T-cell priming by dendritic cells. Proc Natl Acad Sci USA 2011;108:17384–17389.

63 Corcione A, Benvenuto F, Ferretti E et al. Human mesenchymal stem cells modulate B-cell functions. Blood 2006;107:367–372.

64 English K. Mechanisms of mesenchymal stromal cell immunomodulation. Immunol Cell Biol 2013;91:19–26.

65 Maggini J, Mirkin G, Bognanni I et al. Mouse bone marrow-derived mesenchymal stromal cells turn activated macrophages into a regulatory-like profile. PLoS One 2010;5:e9252.

66 Wojtowicz AM, Shekaran A, Oest ME et al. Coating of biomaterial scaffolds with the collagen-mimetic peptide GFOGER for bone defect repair. Biomaterials 2010;31:2574–2582.

67 Shekaran A, Garcia JR, Clark AY et al. Bone regeneration using an alpha 2 beta 1 integrin-specific hydrogel as a BMP-2 delivery vehicle. Biomaterials 2014;35:5453–5461.

68 Moshaverinia A, Chen C, Xu X et al. Bone regeneration potential of stem cells derived from periodontal ligament or gingival tissue sources encapsulated in RGD-modified alginate scaffold. Tissue Eng Part A 2014;20: 611–621.